Early intervention to lower mHTT in the adult zQ175 mouse model results in superior efficacy compared to later intervention.

Jonathan R. Greene[1], Marissa B. Hirst[1], John Obenauer[1], Konstantin Bobkov[1], Mari Aaltonen[2], Joachim Fentz[2], Katharina Hofmann[2], Carleen Kluger[2], Barbara Kracher[2],Tom Schwagarus[2], Jian Chen[3], Jim Rosinski[3], Vahri Beaumont[3]

[1]Rancho BioSciences, San Diego, USA; [2]Evotec SE, Hamburg, Germany; [3]CHDI Management Inc. (the company that manages the scientific activities of CHDI Foundation, Inc.) NY, USA

Introduction

We assessed the relative efficacy of selectively lowering mHTT at different intervention times in a full length heterozygous knock-in mouse model of HD, zQ175DN mice (CHDI-80003019).

Mice were injected intrastriatally with adenovirally-delivered, neuronally expressing ZFP30645, a zinc finger protein (ZFP) repressor targeting expanded CAG repeats in mutant Htt, which resulted in robust and selective abrogation of mHTT production >80% in striatal neurons, or with a control ZFP vector which lacks HTT DNA binding capability (ZFP-DBD). A third 'empty' viral vector was used as an additional control.

Injection of the AAV constructs were undertaken in adult mice either prior to the emergence of any observable pathophysiology at 2 months of age, or at 6 months of age, when mHTT aggregation, neuronal dysfunction and behavioral deficits are well established, but neuronal death is negligible. ZFPs were expressed for 4 and 6 months prior to sacrifice, and striatal tissue was collected for bulk RNA-Seq, snRNA-Seq and proteomic analysis and the results compared across platforms.

Methods

Bilateral simultaneous stereotactic injection of M/F zQ175DN mice (WT and HET)

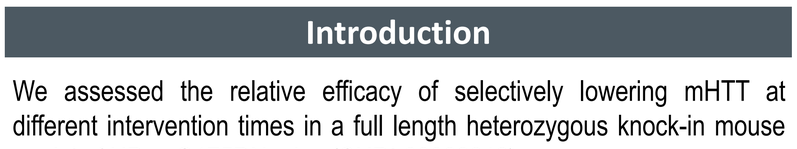

Treatment Groups		Group 1	Group 2	Group 3
		Left: ZFP-30645 Right: ZFP-DBD	Left ZFP- DBD Right: Empty vector (Estop)	Left: Empty vector (Estop) Right ZFP-30645
Injection Age [duration]	**Tissue Collection Age (in Months)**			
2[4]6	WT (M/F)	3/3	3/3	3/3
	zQ175DN HET (M/F)	3/3	3/3	3/3
2[6]8	WT (M/F)	6/6	6/6	6/6
	zQ175DN HET (M/F)	6/6	6/6	6/6
6[4]10	WT (M/F)	3/3	3/3	3/3
	zQ175DN HET (M/F)	3/3	3/3	3/3
6[6]12	WT (M/F)	6/6	6/6	6/6
	zQ175DN HET (M/F)	6/6	6/6	6/6

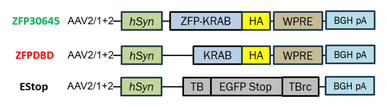

Constructs used : ZFP30645 = active mHTT repressing ZFP 30645, 2 control virus constructs: ZFP-DBD = the inactive DNA binding deleted (DBD) ZFP construct. Estop = "Empty" AAV control construct containing a non-translating 'stuffer sequence'

In-life / Tissue collection: Fig 1 Simultaneous bilateral striatal stereotactic injections of both WT and zQ175 mice were made with 2 of 3 different viral constructs in the matrix design shown. Mice were returned to home cages after surgical recovery and aged for a further 4 or 6 months before striatal tissue collection. Mice were humanely euthanized and striatum (left and right hemisphere) was dissected and rapidly frozen and maintained at -80ºC until processing.

Multiomics profiling

Bulk RNASeq: Hemisphere striatal tissue collected from 2[4]6, 2[6]8, 6[4]10 and 6[6]12 treatment groups (n = 4M/4F samples per each condition) was subjected to RNA isolation and sequencing (Illumina, stranded mRNAseq: 40-50M reads, Paired End, 100-150bp). DESeq2 was used for differential gene expression analysis after sequence alignment and quantification using a custom genome to capture AAV-ZFP marker sequences for infection efficiency (WPRE, BGH pA and ZFP), and Exon1 *Htt1a* transcript was used as a proxy for mHTT lowering efficiency (**Fig 2**). Differentially expressed genes (DEGs)were determined by zQ175 vs WT contrasts (DBD or Estop injected) with a fold change ≥ 1.15, Adjusted P-value < 0.05 (**Fig 3**).

Proteomics: Striatal tissue from 2[6]8 and 6[6]12 treatment groups (n = 3M/3F samples per each condition) was subject to tissue lysis, protein determination, proteolytic digest, TMT 10-plex labeling, reverse-phase chromatography and nano-LC/MS analysis. LC/MS-MS data was analyzed by MaxQuant. Intensity signals for protein groups were normalized by tandem mass tags and converted to log2 scale. Differential expression tests were determined by zQ175 vs WT contrasts (DBD or Estop injected) and were performed using the Limma package in R. Proteins with fewer than 2/3 (8 out of 12) measured values were filtered out. Differentially expressed proteins (DEPs) were determined by zQ175 vs WT contrasts (DBD or Estop injected) with a fold change ≥ 1.15, Adjusted P-value < 0.1 DEPs were selected as the union of protein lists from two independent analyses **(Fig 4).**

snRNASeq: Nuclei from striatal tissue hemisphere punches from 2[4]6, 2[6]8, 6[4]10 and 6[6]12 treatment groups (n = 2M/2F samples per each condition) were recovered by sample lysis followed by two density gradient centrifugations to sample purity >97%. RNA was isolated and sequencing performed (Novaseq 6000 snRNAseq Platform, CeGAT). Ambient RNA determination and filtering was conducted using SoupX and CellBender. The intersection of retained cells using both approaches were processed initially in Scarf, and partial PCA (pPCA) was used for batch correction. Seurat was used to process the data . Cell type classification used SVM from a previous snRNA-Seq striatal study. For HD signature reversal analysis, data were rolled up into "pseudobulk" by sample replicate, treatment and scenario and then DESeq2 was used for HD Signature and Treatment contrasts. To identify DEGs / reversals only in neurons infected by ZFP and subject to HTT lowering, ZFP30645 and ZFP-DBD treated samples were filtered to retain neuronal cell types with WPRE normalized expression >0.5. Conversely, to unambiguously assess the impact of neuronal HTT-lowering on non-neuronal HD signature rescues, astrocytes and oligodendrocyte cells were filtered to only retain cells with no WPRE expression (normalized expression <0.5). (**Fig 5**)

Omics Reversal/Rescue/Prevention Analysis: Starting with "Disease Contrast" and "Treatment Contrast" results from differential expression analysis, we used a Bayesian method described in Marchionini *et al*, *JCI Insight*, 2022 (PMID 36278490) to calculate the probability that zQ175DN Disease signature DEGs / DEPs returned towards WT levels with ZFP30645 administration, as well as a classification of the reversal efficiency (super (S), full (F) partial (P) or negligible (N) reversal). Generally, disease reversals were largely equivalent regardless of whether the control contrast used was ZFP-DBD or Estop. For simplicity, only ZFP-DBD control contrast results are shown throughout. (**Fig 6 – 9**)

Results

Confirmation of ZFP expression and mHTT lowering

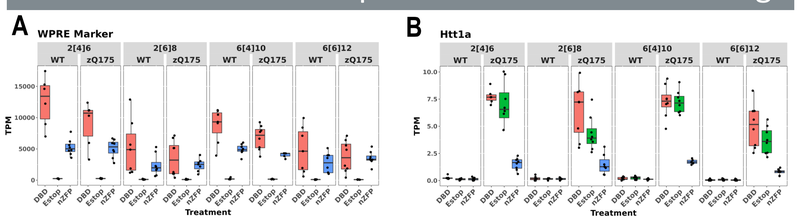

Figure 2: A custom gene model was used to examine viral expression levels (ie: WPRE, ZFP, DBD domain), and mHTT reduction from bulk RNAseq. **A**: shows expression level detection for the vector AAV WPRE marker sequence. **B**: shows *HTT1A* (HTT Intron 1) transcript levels as a proxy for mHTT, which was elevated in Q175 v WT, and effectively reduced by ZFP30645 expression across all ages examined.

zQ175DN v WT "HD signatures" across the 3 Platforms

RNAseq (bulk striatal tissue)

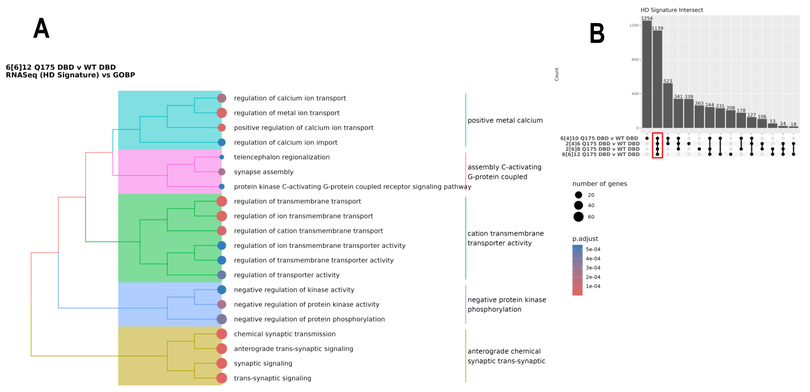

Figure 3: >2000 'HD disease signature' DEGs were identified in control vector (ZFPDBD –injected) zQ715DN v WT striatal tissue across all ages queried (6,8,10 and 12 months)
A: GOBP gene sets that are overrepresented in DEGs from 12-month-old Q175DN v WT (ZFPDBD-injected) mice, identified using GSEA and clustered by overlapping gene composition.
B. Disease signature DEGs were well conserved across all ages queried (6,8,10,12 months).
Q175DN v WT (Estop injected) mice showed equivalent results (data not shown)

Proteomics (bulk striatal tissue)

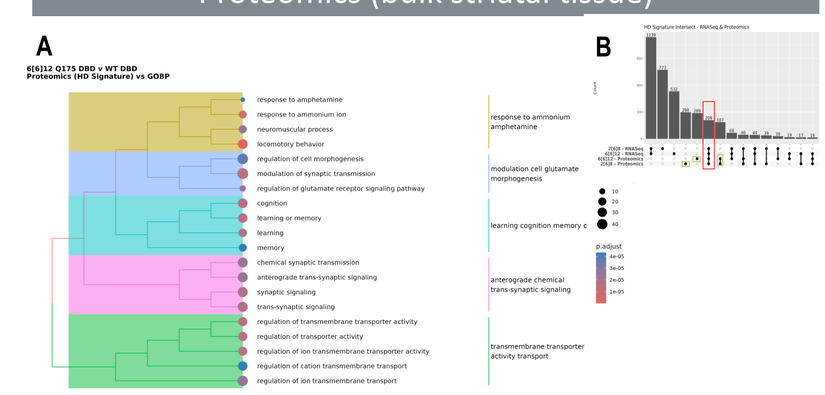

Figure 4: **>1000 'HD disease signature' DEPs were identified in control vector (ZFPDBD–injected) zQ715DN v WT striatal tissue at 8 and 12 months**
A GOBP gene sets that are overrepresented in DEPs from 12-month-old Q175DN v WT (ZFPDBD-injected) mice, identified using GSEA and clustered by overlapping gene composition. Note that there are many shared characteristics with results shown above for RNASeq HD signatures.
B Overlap between individual DEGs and DEPs. There were 209 DEGs/DEPs in common between all datasets (red box), but ~ 40% of total DEPs identified were not predicted from RNAseq DEGs (green boxes).

snRNAseq (striatal cell type DEGs)

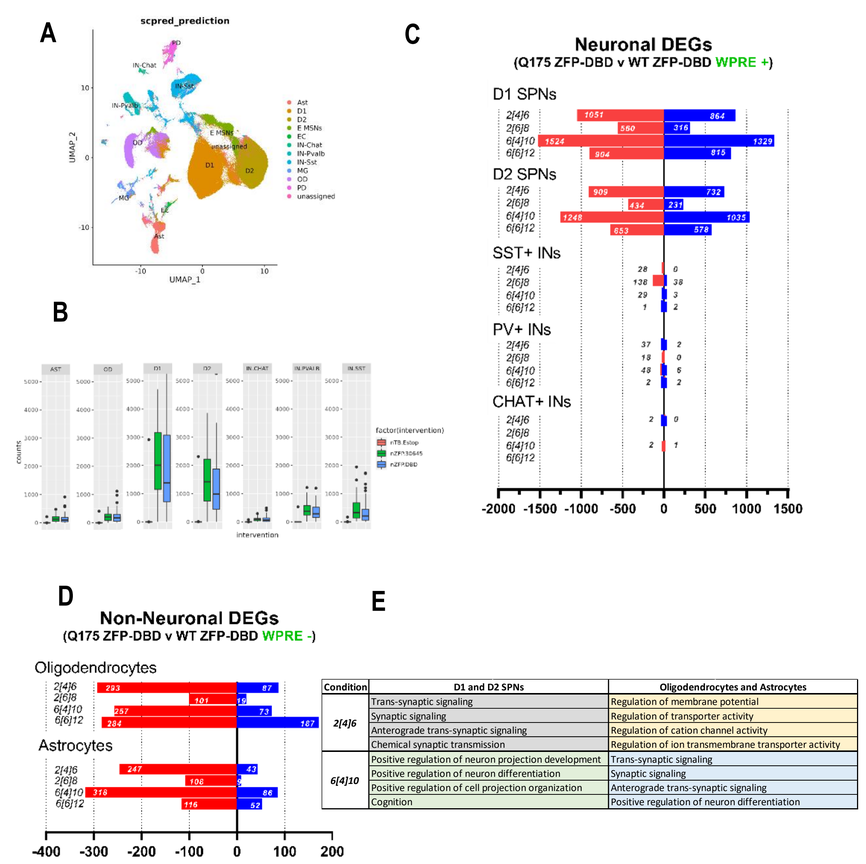

Condition	D1 and D2 SPNs	Oligodendrocytes and Astrocytes
2[4]6	Trans-synaptic signaling	Regulation of membrane potential
	Synaptic signaling	Regulation of transporter activity
	Anterograde trans-synaptic signaling	Regulation of cation channel activity
	Chemical synaptic transmission	Regulation of ion transmembrane transporter activity
6[4]10	Positive regulation of neuron projection development	Trans-synaptic signaling
	Positive regulation of neuron differentiation	Synaptic signaling
	Positive regulation of cell projection organization	Anterograde trans-synaptic signaling
	Cognition	Positive regulation of neuron differentiation

Figure 5: Cell type specific DEGs determined by snRNAseq
A: UMAP coordinates overlaid with cell type classification post-SVM. **B**: A custom genome was used to capture WPRE sequence expression evaluated over cell types, to determine putatively infected (WPRE+) v non-infected (WPRE-)cells. ZFP constructs expressed prominently in D1 and D2 MSNs, as well as to al lesser extent in other rarer neuronal cell populations. Non-neuronal cell types showed minimal expression of AAV-ZFP30645 or DBD constructs as expected with a human synapsin promoter, although some ectopic expression was detected. **C** Q175 v WT DEGs for D1, D2 MSNs and interneurons, *filtered to include only those neurons with detectable expression of WPRE >0.5)*. D1 and D2 MSNs have the greatest HD signature, while detected dysregulated gene signatures in interneuron populations were minimal. **D**: oligodendrocytes and astrocyte DEGs were calculated from cells with WPRE expression <0.5 (ie non-infected). **E**: Of the top 5 enriched gene sets per cell type dysregulated between Q175 and WT @ 6 and 10 months of age, 4/5 are in common to both D1& D2 MSNs, and 4/5 were in common to both oligodendrocytes & astrocytes (GOBP:GSEA).

Prevention / Rescue of Disease signatures by ZFPs

ZFP30645-induced rescue : RNAseq and Proteomics

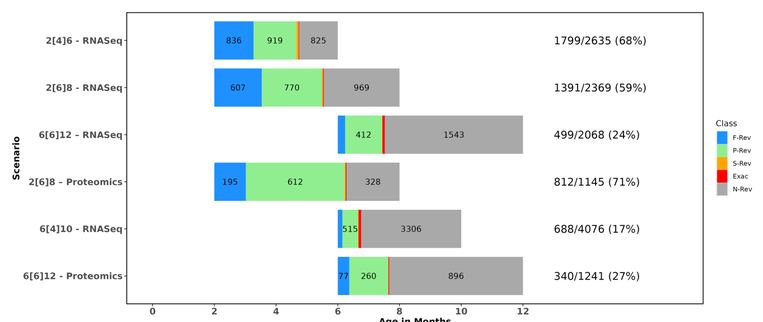

Figure 6: Prevention/rescue probabilities and classifications were determined for bulk RNASeq and Proteomics scenarios. We used the method described in Marchionini, et al, 2022; comparing the ability of ZFP-30645 to rescue Q175 DEGs / DEPs (ZFP30645 v ZFP-DBD reversal scenario). For each scenario, the bar plot spans the treatment time and indicates the number of Full (F-Rev), Partial (P-Rev), Super (S-Rev) and Negligible (N-Rev) preventions/rescues, as well as Exacerbations (Exac). Numbers to the right indicate the overall number of reversals (F-Rev + P-Rev + S-Rev) divided by the number of HD Signature genes/proteins, as well as the resulting percentage. Early intervention resulted in ~ 70% rescue of the HD signature in both RNAseq and proteomic datasets. In contrast, if intervention was started at 6 moths of age, rescue was greatly diminished, with only approximately 20-30% of the HD signature now responsive to reversal following HTT lowering.

ZFP-30645-induced rescue of neuronal signatures : snRNAseq

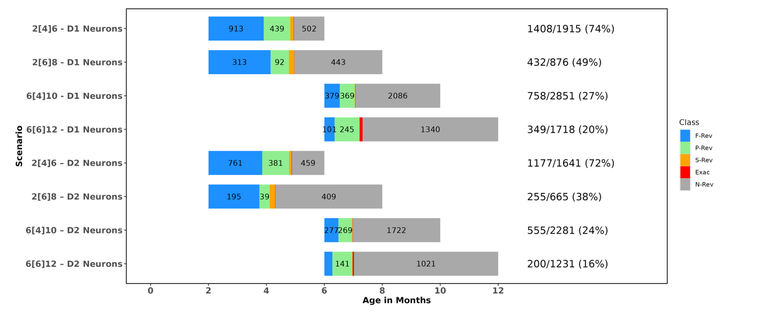

Figure 7: A. Cell-specific D1 MSN, D2 MSN prevention/rescue probabilities and classifications were determined from snRNASeq 'psuedobulk' data as described in Figure 6. Consistent with bulk RNAseq and proteomic data, ZFP30645 was much more effective when administered at 2 months of age, prior to the emergence of any observable pathophysiology than when administered at 6 months when mHTT aggregation, neuronal dysfunction and behavioral deficits are well established. Reversals were calculated only for D1 and D2 SPNs whose normalized WPRE expression levels were >0.5, indicating effective ZFP expression in all cells queried.

Astrocyte and Oligodendrocyte reversals: snRNAseq

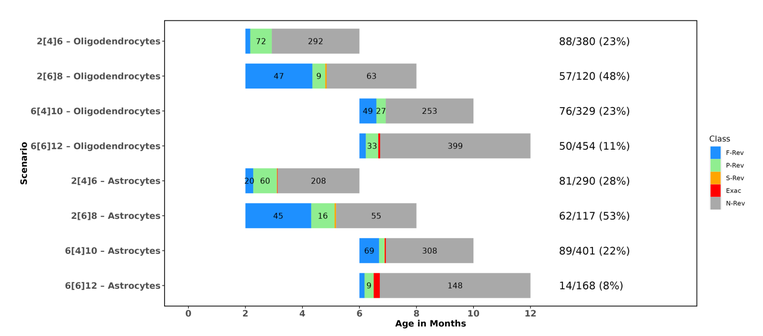

Figure 8: To determine the impact that neuronal HTT lowering had on non-neuronal cell types, cell-specific astrocyte and oligodendrocyte prevention/rescue probabilities and classifications were determined as described in Figure 6. In this instance, reversals were calculated only for cells whose normalized WPRE expression levels were <0.5 (ie non-infected non-neuronal cells). Astrocytes and oligodendrocytes appeared to benefit from neuronal HTT lowering / restoration of neuronal health, indicating that their transcriptional changes are in part driven in response to mHTT-mediated neuronal dysfunction, and rectified following neuronal mHTT lowering, as previously described for astrocytes (Gangwani *et al, Cell Reports*, 2023, PMID 36640336). With early intervention, we found that both oligodendrocyte and astrocyte HD signatures were restored by ~25 – 50%, dependent on duration of intervention. This was less effective if treatment start was delayed, with reversals dropping to ~10 – 20% across both cell types.

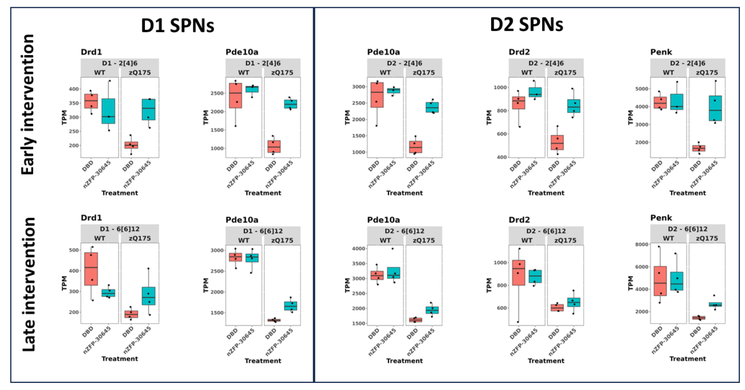

Figure 9 Biomarker (PET ligand / CSF Immunoassay) candidate mRNA rescues. Rescue of dopamine D1 and D2 receptor, PDE10 (PET candidates) and proenkephalin (CSF immunoassay candidate) -encoding mRNAs by ZFPs, as a guide to likely responsiveness to mHTT lowering intervention. The diminished rescues following late administration at 6 months highlight how timing of intervention influences effect size.

Conclusions and Next Steps

- Timing of ZFP mHTT lowering therapies affects outcome.
  - Our results using striatal bulk RNAseq profiling, bulk proteomic profiling, and snRNAseq analysis show that early ZFP30645 intervention to lower mHTT shows ≥2-fold efficacy compared to late intervention paradigms across all platforms.
- These data have implications for expected effect size in clinical trials. Our ultimate aim is to build interpretable bridges to inform on optimal intervention times.
  - Our data can be interrogated to guide potential candidate biomarker efficacy / effect sizes for therapeutic strategies, and may also drive novel identification of promising biomarker candidates
- Our current efforts are focused on a better mechanistic understanding of why later intervention times are less effective, even in the absence of overt striatal cell atrophy, as described here
  - Two hypotheses currently being pursued are that 1) diminished responsiveness to mHTT lowering late in disease pathology may be due to an inability to clear nuclear aggregate pathology and/or 2) occurs as a result of epigenetic state switching, rendering transcriptional deregulation refractory to intervention.